Observation of optical torsional stiffness in a high optical power cavity

Yaohui Fan,[1,a)] Lucienne Merrill,[1] Chunnong Zhao,[1] Li Ju,[1] David Blair,[1] Bram Slagmolen,[1,b)] David Hosken,[2] Aidan Brooks,[2,c)] Peter Veitch,[2] Damien Mudge,[2] and Jesper Munch[2]
[1]*School of Physics, University of Western Australia, 35 Stirling Highway, Crawley, Western Australia 6009, Australia*
[2]*Department of Physics, The University of Adelaide, Adelaide, South Australia 5005, Australia*

(Received 6 January 2009; accepted 4 February 2009; published online 24 February 2009)

We have observed negative optical torsional rigidity in an 80 m suspended high optical power cavity that would induce the Sidles–Sigg instability as a result of sufficient circulating power. The magnitude of the negative optical spring constant per unit power is a few μN m/W as the result of the optical torsional stiffness in the yaw mode of a suspended mirror Fabry–Pérot cavity. It has been observed to depend on the g-factor of the cavity which is in agreement with the Sidles–Sigg theory. © *2009 American Institute of Physics*. [DOI: 10.1063/1.3088850]

Around the world, there are several kilometer long suspended Michelson interferometers, with Fabry–Pérot (FP) cavities in each arm, aimed at detecting gravitational waves. Effort is underway to improve these interferometers, minimizing the effect of noise sources which contaminate the gravitational wave readout channel. Quantum shot noise is one source which affects the sensitivity of the detectors. The simplest way to reduce this noise is to increase the optical power within the FP cavities of the interferometer. An upgrade to LIGO interferometers includes increasing the optical power circulating in the FP cavities to 830 kW.[1]

An increase in the optical power within an optical cavity directly increases the radiation pressure, thereby increasing the optomechanical coupling. This can act in both longitudinal and torsional degrees of freedom. Higher power within the cavity changes both the suspended mirror pendulum mode stiffness and the torsional mode stiffness, causing them to act like two strongly coupled oscillators.[2] The longitudinal optical spring effects within optical cavities, as a result of this pendulum mode optical stiffness, have been observed and extensively studied.[3–10] The optical spring can also induce instabilities or passive cooling of the internal mechanical modes of the cavity end mirrors through coupling to cavity high order modes.[5]

In addition to the longitudinal optical spring effects on an optical cavity, large circulating optical power can also couple the torsional mode of the test mass suspension to the optical mode. This effect was first recognized by Solimeno *et al.*[11] in 1991. They analyzed the phenomena for a cavity consisting of one suspended mirror and one fixed mirror using a modal formalism. Some years later, Sidles and Sigg extended this analysis to a cavity with two suspended mirrors using a simplified geometric formalism, and they found that their results remained consistent with Solimeno *et al.*[11]

Sidles–Sigg (SS) theory predicts that optically induced, negative torsional stiffness could potentially be large enough to overcome the stiffness of the mirror suspensions, introducing an angular instability within the cavity of the interferometers. These instabilities depend upon the circulating power, cavity finesse and linewidth, and the detuning between the laser frequency and the cavity resonant frequency. SS theory indicates that choosing negative mirror g-factors (i.e., near concentric cavities) maximizes the critical circulating power at which the cavity becomes unstable.

Driggers[12] observed the optical torsion stiffness in a suspended three mirror mode cleaner cavity and its dependency on the circulating power. In this letter we present results on the cavity g-factor dependence of optical torsional stiffness in a two mirror cavity. Our results are in agreement with the SS geometric formalism model. Figure 1 reviews the SS geometric model below.

As shown in Fig. 1, we assume that the optical cavity is initially well aligned and that the cavity mode is located at the center of the mirror. Any suspended mirror angular misalignment will cause the cavity mode to walk away from the center of the mirror. The displacement of the mode from the center of the mirror causes the radiation pressure of the laser beam stored inside the cavity to introduce a torque on each end mirror, modifying the dynamics of the suspended mirror.

The differential equations describing the dynamics of the suspended mirror are

$$\frac{d^2}{dt^2}\alpha_1 = -\omega_1^2\alpha_1 + \frac{2P}{cI_1}\left(\frac{g_2}{1-g_1g_2}L\alpha_1 + \frac{1}{1-g_1g_2}L\alpha_2\right),$$

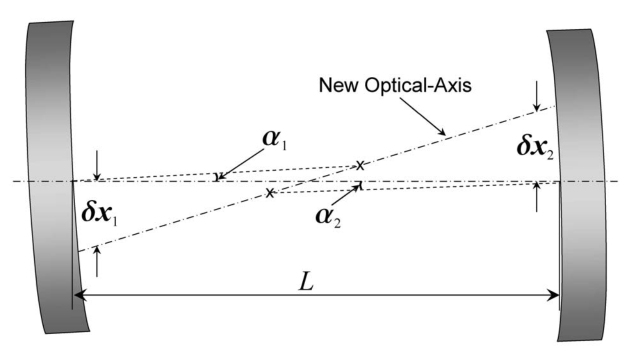

FIG. 1. FP cavity with tilted mirrors, where L is the length of the cavity, α_1 and α_2 are the misalignment angles for their corresponding mirrors, and δx_1 and δx_2 are the mode position offsets.

[a)]Tel.: +61 8 6488 4551. Electronic mail: fanyh@physics.uwa.edu.au.
[b)]Present address: Centre for Gravitational Physics, the Australian National University, Canberra, Australia.
[c)]Present address: Caltech, Pasadena, California, USA.

TABLE I. Parameters of the cavity.

	Input mirror	End mirror	Compensation plate
Radius of curvature (m)	$R_1=\infty$	$R_2=790$	Flat
Materials	Sapphire	Sapphire	Fused silica
Diameter (mm)	100	150	160
Thickness (mm)	46	80	17
$\omega_{1\text{pitch}}$ (Hz)	0.81	⋯	⋯
$\omega_{1\text{yaw}}$ (Hz)	0.65	⋯	⋯
Cavity length (m)	80		

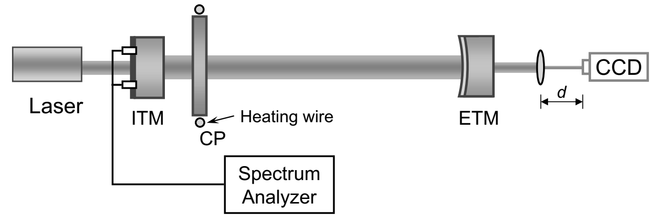

FIG. 2. The schematics of the experimental setup, where the ITM is the input mirror, ETM is the end mirror, d is the distance between the end mirror and the CCD camera, and CP is the thermal CP.

$$\frac{d^2}{dt^2}\alpha_2 = -\omega_2^2\alpha_2 + \frac{2P}{cI_2}\left(\frac{1}{1-g_1g_2}L\alpha_1 + \frac{g_1}{1-g_1g_2}L\alpha_2\right), \quad (1)$$

where P is the circulating power in the cavity, L is the length of the cavity, α_i, I_i, and ω_i are the misalignment angles, moments of inertia and resonant frequency for each mirror, respectively, and the g-factor for each mirror is defined as $g_i=1-L/R_i$.

By inspecting Eq. (1), and increasing the optical power, we can see that the two cavity mirrors are no longer independent (α_1 and α_2 are present in both equations), but instead are connected together by the radiation pressure of the laser light circulating inside the cavity.

In the experiments described here (Table I), the moment of inertia of the end mirror is more than 10 times larger than that of the input mirror, also it should be noted that the end mirror is heavily damped. Under these conditions, it is a good approximation to consider the end mirror fixed and well aligned, then $\alpha_2=0$.

The negative torsional optical spring constant is,

$$k_{\text{op}} = -I\Omega^2 = -I\frac{2P}{cI_1}\frac{g_2}{1-g_1g_2}L, \quad (2)$$

where Ω is the resonant frequency of the optical spring and I equals to I_1. From Eq. (2) we can see how strong the optical spring constant is as a function of positive mirror g-factors. If the cavity g-factor is increased, we should find that the absolute value of the negative optical spring constant is also increased.

When the circulating power P reaches a level where $\omega_1=\Omega$, the system approaches instability. We define this power as the critical power P_c,

$$P_c = \frac{cI_1\omega_1^2}{2L}\frac{1-g_1g_2}{g_2}. \quad (3)$$

With the parameters of the cavity listed in Table I, the critical power $P_{c(\text{yaw})}=4.5$ kW and $P_{c(\text{pitch})}=7.0$ kW. Our cavity has a relatively stiff torsional suspension, so the critical power is quite large.

The negative optical spring can be evaluated by measuring the effective resonant frequency of the input mirror. The effective resonant frequency of the input mirror should be,

$$\omega_{\text{eff}} = \sqrt{\omega_1^2-\Omega^2}. \quad (4)$$

The experiment described here was performed at the Gingin High Optical Power Facility in Western Australia.[13] Figure 2 shows the experimental layout. A ~3 W neodymium doped yttrium aluminum garnet (Nd:YAG) laser is injected and phase-locked into the FP cavity, which consists of an input test mass (ITM) and an end test mass (ETM). The test masses are supported by simple wire loop pendulums which are driven by seismic noise, and controlled by conventional light-emitting diode (LED) photodiode shadow sensors.[14] An intracavity low absorption thermal compensation plate (CP) is placed close to the ITM, and tunes the mirror g-factor g_1 by electrically heating the CP's cylindrical surface (i.e., introducing a negative thermal lens). The charge-coupled device (CCD) camera located behind the ETM measures the transmitted beam profile.[15]

We measured the resonant frequency $\omega_{1\text{yaw}}$ of the ITM yaw degree of freedom as a function of the total cavity g-factor, which was varied by thermal tuning the focal length of the CP. The spectrum analyzer, shown in Fig. 2, measured the resonant frequency of the ITM, from which we calculated the value of the negative optical spring constant from Eq. (2). This measurement was difficult to obtain for several reasons. First, thermal tuning required at least 1 h to reach thermal equilibrium due to the low thermal absorption and conductivity of the fused silica substrate of the CP. Second, the torsional mode measurement required either switching off the local control system or keeping the local control loop closed by injecting a significantly larger amplitude signal than that of seismic noise. In either case, the ITM would swing in a large amplitude driven by seismic noise or the injection signal. ITM fluctuations occasionally caused power loss in the cavity which decreased the optical spring effect. Long integration times, required for precision measurements, made our cavity more susceptible to seismic noises which caused the cavity to lose lock, especially when we had a high g-factor cavity.

The cavity g-factor can be determined by two methods. One is through measuring the transmitted beam size by the CCD camera shown Fig. 2.[15] Another way is to measure the mode spacing Δf between the first-order mode and the fundamental mode of the cavity. The cavity g-factor can be expressed as[16]

$$g = \cos^2\left(\frac{\pi\Delta f}{\text{FSR}}\right), \quad (5)$$

here FSR is the free spectral range of the cavity. The first-order mode frequency was obtained by phase-modulating the incident laser with a swept signal.

Figure 3 shows the negative spring constant divided by the power P as a function of the cavity g-factor as compared with the calculated values using Eq. (2). The power P was calculated from the transmitted beam power on the CCD camera. The measured frequency shift for ITM yaw mode is ~30 MHz with about 2.1 W incident power (~630 W circulating power). The cavity g-factors were obtained using equation Eq. (5) by measuring the cavity mode spacing. When the cavity was locked and the local control system was

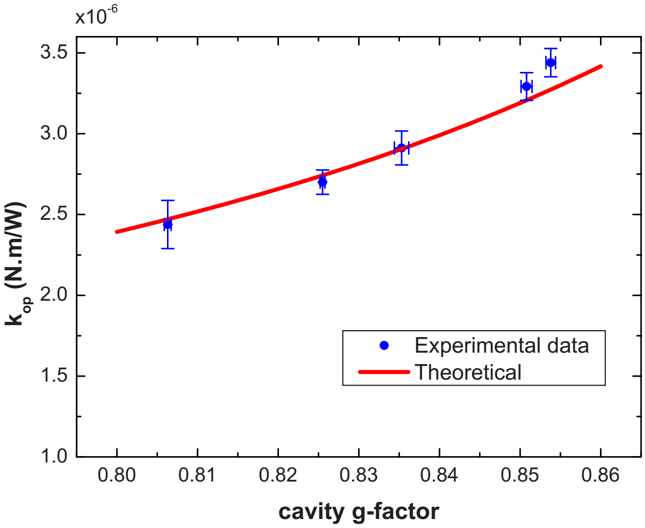

FIG. 3. (Color online) The negative torsional optical spring constant k_{op} for the ITM yaw mode as a function of the cavity g-factor. The spring constant has been normalized by dividing by the circulating power.

on, the cavity mode spacing varied from ~190 to ~140 kHz at different CP heating powers. At certain CP heating powers we turned off the ITM local control and measured the yaw mode resonant frequency shift due to the optical torsional stiffness. From the frequency shift we calculated the optical torsional stiffness.

As seen in Fig. 3, the measured data agrees relatively well with calculated data. The error bars shown in the graph were statistical errors from measurements taken under the same conditions. At higher cavity g-factors, the cavity alignment fluctuated a great deal at the yaw mode resonant frequency (~0.6 Hz). The frequency shift measurements took about 400 s, this averaged out the fluctuation and the statistical errors did not increase with the increased fluctuation at higher cavity g-factors. However, the instantaneous power fluctuation, which changes the average power level, would not affect the frequency shift during the measurement time due to the high Q-factor ($\sim 10^4$) of the yaw mode. Therefore when we used the average power to calculate the unit power optical spring constant, using Eq. (2), the average power level could have been underestimated at high cavity g-factors, leading to the deviations as seen in Fig. 3.

In conclusion, we have observed the optical torsional stiffness in an 80 m high optical power cavity. The magnitude of the optical spring effect is much smaller in a cavity with concentric mirrors and it should be noted that the design for the next generation of high-power laser interferometers have taken this instability into consideration and modified their optical cavities from nearly planar to nearly concentric.

This experiment was developed in collaboration between the Australian Consortium for Gravitational Astronomy and the U.S. LIGO Laboratory. We would like to thank the International Advisory Committee of the Gingin Facility for their encouragement and advice, and the center of gravitational physics of the Australian National University for useful discussions and for providing cavity locking electronics. This research was supported by the Australian Research Council and the Department of Education, Science and Training by the U.S. National Science Foundation (NSF Grant Nos. PHY-0555453 and 0PHY-757968.

[1]P. Fritschel, Advanced LIGO Systems Design, http://www.ligo.caltech.edu/docs/T/T010075-00.pdf.
[2]J. A. Sidles and D. Sigg, Phys. Lett. A **354**, 167 (2006).
[3]A. Dorsel, J. D. McCullen, P. Meystre, E. Vignes, and H. Walther, Phys. Rev. Lett. **51**, 1550 (1983).
[4]V. B. Braginsky, S. E. Strigin, and S. P. Vyatchanin, Phys. Lett. A **287**, 331 (2001).
[5]C. Zhao, L. Ju, J. Degallaix, S. Gras, and D. G. Blair, Phys. Rev. Lett. **94**, 121102 (2005).
[6]B. S. Sheard, M. B. Gray, C. M. Mow-Lowry, and D. E. McClelland, Phys. Rev. A **69**, 051801 (2004).
[7]S. Gigan, H. R. Böhm, M. Paternostro, F. Blaser, G. Langer, J. B. Hertzberg, K. C. Schwab, D. Bäuerle, M. Aspelmeyer, and A. Zeilinger, Nature (London) **444**, 67 (2006).
[8]A. Schliesser, P. Del'Haye, N. Nooshi, K. J. Vahala, and T. J. Kippenberg, Phys. Rev. Lett. **97**, 243905 (2006).
[9]O. Arcizet, P.-F. Cohadon, T. Briant, M. Pinard, and A. Heidmann, Nature (London) **444**, 71 (2006).
[10]T. Corbitt, Y. Chen, E. Innerhofer, H. Müller-Ebhardt, D. Ottaway, H. Rehbein, D. Sigg, S. Whitcomb, C. Wipf, and N. Mavalvala, Phys. Rev. Lett. **98**, 150802 (2007).
[11]S. Solimeno, F. Barone, C. de Lisio, L. Di Fiore, L. Milano, and G. Russo, Phys. Rev. A **43**, 6227 (1991).
[12]J. Driggers, Optomechanical alignment instability in LIGO mode cleaners, http://www.ligo.caltech.edu/docs/T/T060240-00.pdf.
[13]B. J. J. Slagmolen, Proceedings of the Australian Consortium for Interferometric Gravitational Astronomy (ACIGA) Workshop, Perth, Australia, April 2004 (unpublished).
[14]N. Mavalvala, LHO 2 km arm cavity tests: Suspensions, http://www.ligo.caltech.edu/docs/G/G000114-00.pdf.
[15]C. Zhao, J. Degallaix, L. Ju, Y. Fan, D. G. Blair, B. J. J. Slagmolen, M. B. Gray, C. M. Mow Lowry, D. E. McClelland, D. J. Hosken, D. Mudge, A. Brooks, J. Munch, P. J. Veitch, M. A. Barton, and G. Billingsley, Phys. Rev. Lett. **96**, 231101 (2006).
[16]H. Kogelnik and T. Li, Appl. Opt. **5**, 1550 (1966).